

## Near-Earth Asteroids in Spitzer Observations

This is a brief discussion of near-Earth asteroid (NEA) counts in Spitzer Space Telescope observations. The approach is similar to a previous discussion of main-belt asteroids.

### Background:

Spitzer will be remarkably sensitive to any NEA found in the field of its mid-infrared instruments, especially the IRAC 8  $\mu\text{m}$  filter. It can detect an asteroid with a diameter as small as  $\approx 10$  meters at 0.2 AU from the Earth at 8  $\mu\text{m}$ . However, it is unlikely to find a bright NEA in an arbitrary field as shown in the simulation below.

### Size distribution:

We averaged recent estimates of the number of NEAs (Rabinowitz *et al.* 1994; Rabinowitz *et al.* 2000; Stuart 2001) and approximated the cumulative size distribution of the NEAs with a single power law:

$$N(> D) = 1000 \left( \frac{1}{D} \right)^{2.0}$$

where  $D(\text{km})$  is the asteroid diameter. This should give numbers reliable to within a factor 6 down to a diameter of 10 meters.

### The near-Earth asteroid simulation:

The positions and fluxes of  $10^7$  NEAs with diameters larger than 10 meters were simulated with a Monte Carlo model. The distributions of orbital elements  $a$ ,  $e$ , and  $i$  were taken from Rabinowitz *et al.* (1994). The other orbital elements were randomly assigned.

Infrared fluxes were estimated with the standard thermal model for asteroids (Lebofsky and Spencer 1989). The adopted average Bond albedo was  $A = 0.05$ . The thermal emissivity was  $\epsilon = 1.0$ . The assumed infrared beaming factor was  $\eta = 1.2$  (Harris 1998), which may be the most reasonable value for the small bodies of interest here.

Reflected light contributes moderately to the flux in the IRAC 3.6  $\mu\text{m}$  band, and weakly at 4.5  $\mu\text{m}$ . We assume an average geometric albedo of 0.1 (very uncertain) and a phase law like that at visible wavelengths (Bowell *et al.*, 1989).

The numbers of main-belt and near-Earth asteroids brighter than a given flux limit are shown in Figure 1 for a typical Spitzer field-of-view. Power-law fits to the results of the simulations are plotted to account for the numerical limitations of the simulations.

Though they are on average closer, hotter, and have a wider spread in inclination than main-belt asteroids, the fact that the NEAs are a factor  $\approx 800$  down by number makes them much less of a concern than main-belt asteroids, except at high ecliptic latitudes, where the numbers are low.

Also plotted are some typical rates of motion in ecliptic coordinates (Figure 2).

**Credits:**

Prepared under the auspices of the Spitzer Science Center by T.Y. Brooke, to whom questions or comments can be addressed: tyb@phobos.caltech.edu.

**References:**

- Bowell, E., Hapke, B., Domingue, D., Lumme, K., Peltoniemi, J., and Harris, A. 1989, in *Asteroids II*, ed. R.P. Binzel, T. Gehrels, and M.S. Matthews, Univ. of Ariz. Press, Tucson, p. 524.
- Harris, A.W. 1998, *Icarus*, **131**, 291.
- Lebofsky, L.A. and Spencer, J.R. 1989, in *Asteroids II*, ed. R.T. Binzel, T.Gehrels, and M.S. Matthews, Univ. of Arizona Press, Tucson, p. 128.
- Rabinowitz, D., Bowell, E., Shoemaker, E., and Muinonen, K. 1994, in *Hazards due to Comets and Asteroids*, ed. T. Gehrels, Univ. of Ariz. Press, Tucson, pp. 285-312.
- Rabinowitz, D., Helin, E., Lawrence, K., and Pravdo, S. 2000, *Nature*, **403**, 165.
- Stuart, J.S. 2001, *Science*, **294**, 1691.

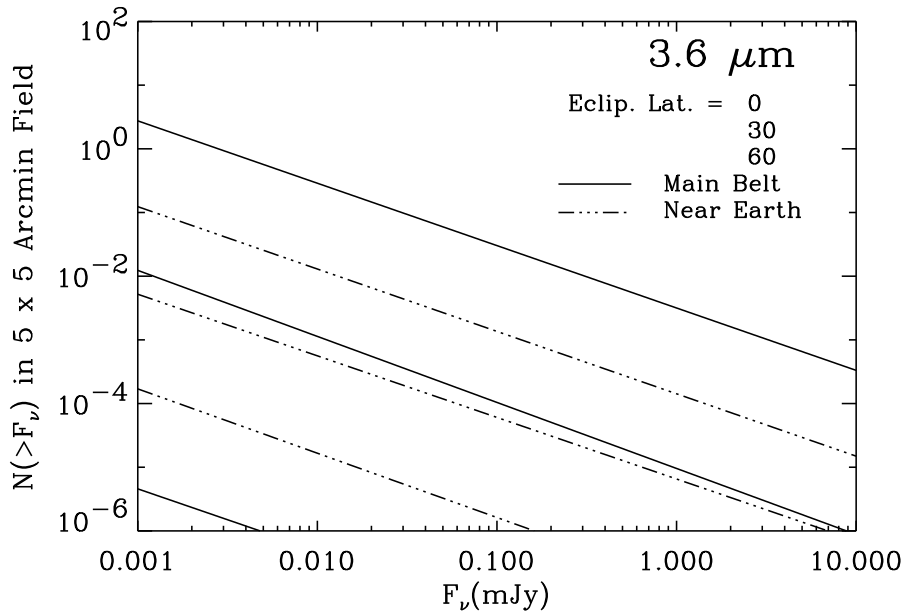


Fig. 1(a) - Cumulative main-belt (solid lines) and near-Earth (dash-dot lines) asteroids brighter than  $F_\nu$  in a  $5' \times 5'$  area for various ecliptic latitudes at a wavelength of  $3.6 \mu\text{m}$ . Curves are power-law fits to the results of the Monte Carlo simulations.

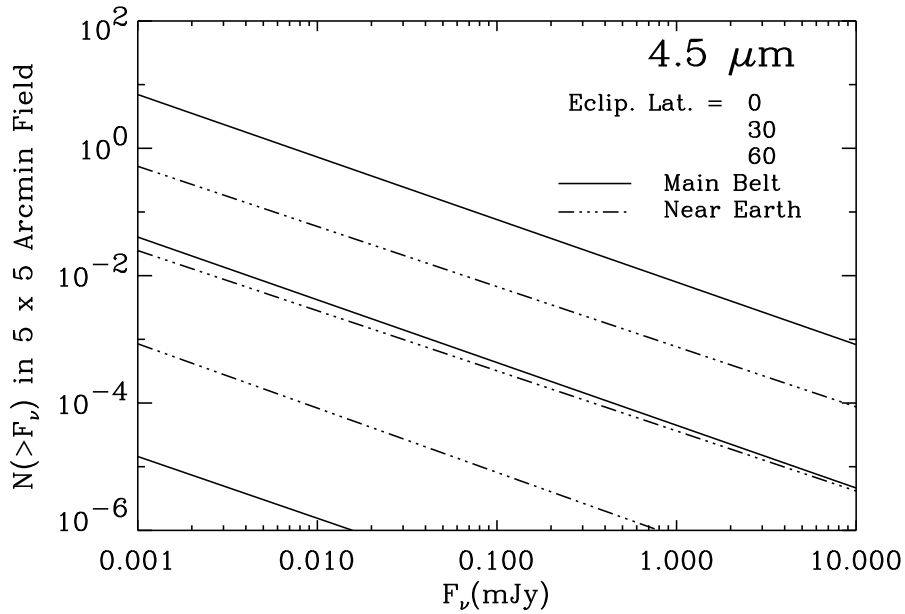


Fig. 1(b) - Same as Fig. 1(a) at  $4.5 \mu\text{m}$ .

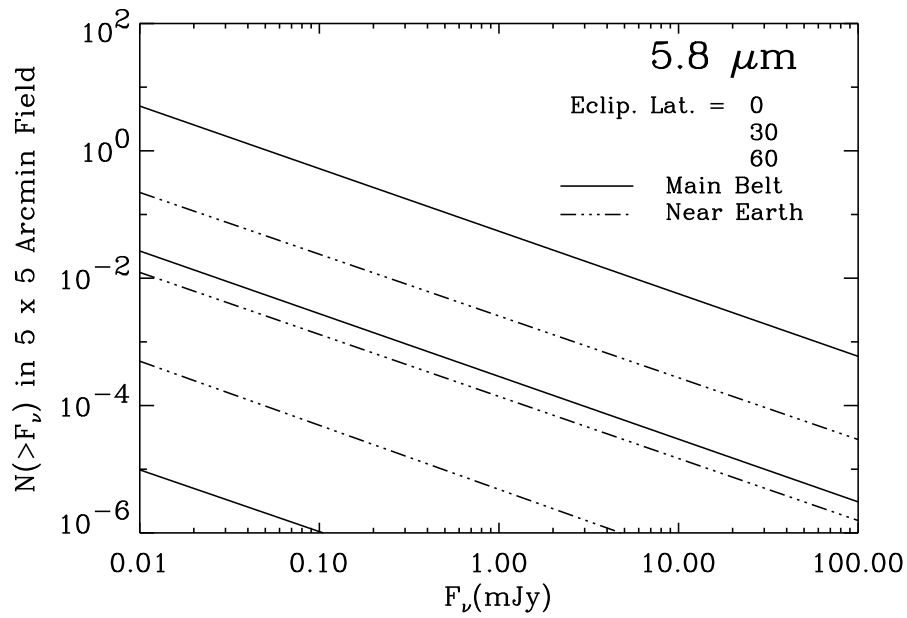


Fig. 1(c) - Same as Fig. 1(a) at 5.8  $\mu\text{m}$ .

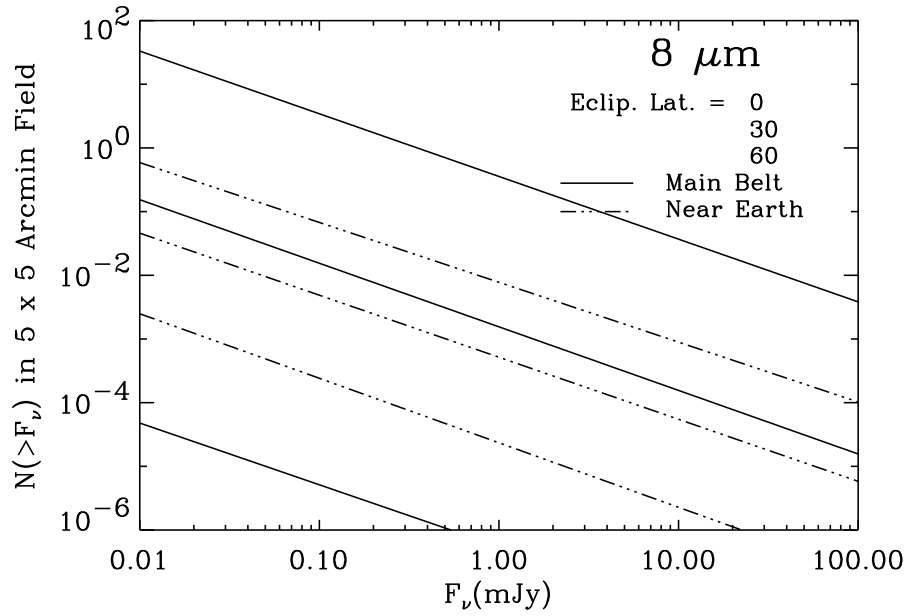


Fig. 1(d) - Same as Fig. 1(a) at 8  $\mu\text{m}$ .

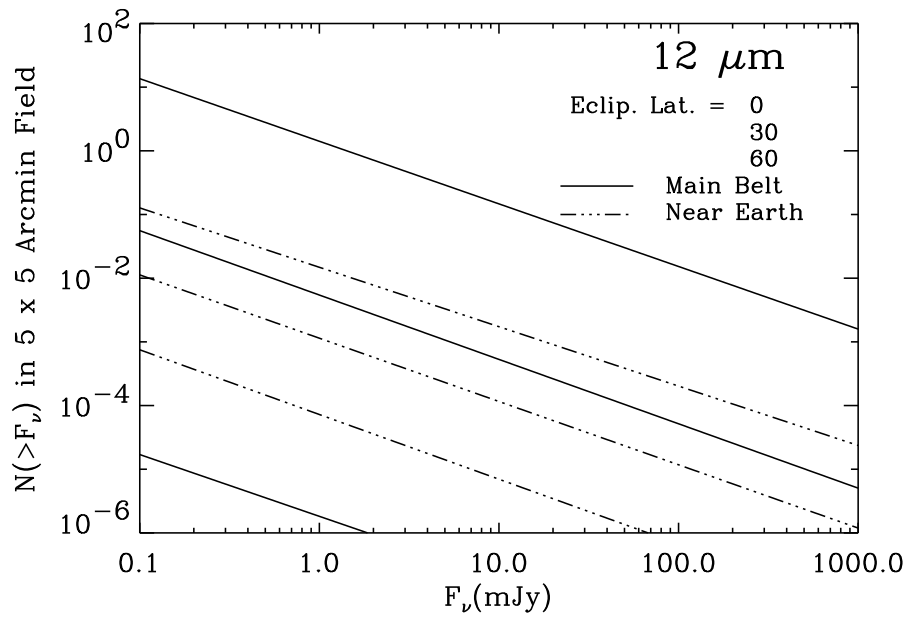


Fig. 1(e) - Same as Fig. 1(a) at 12  $\mu\text{m}$ .

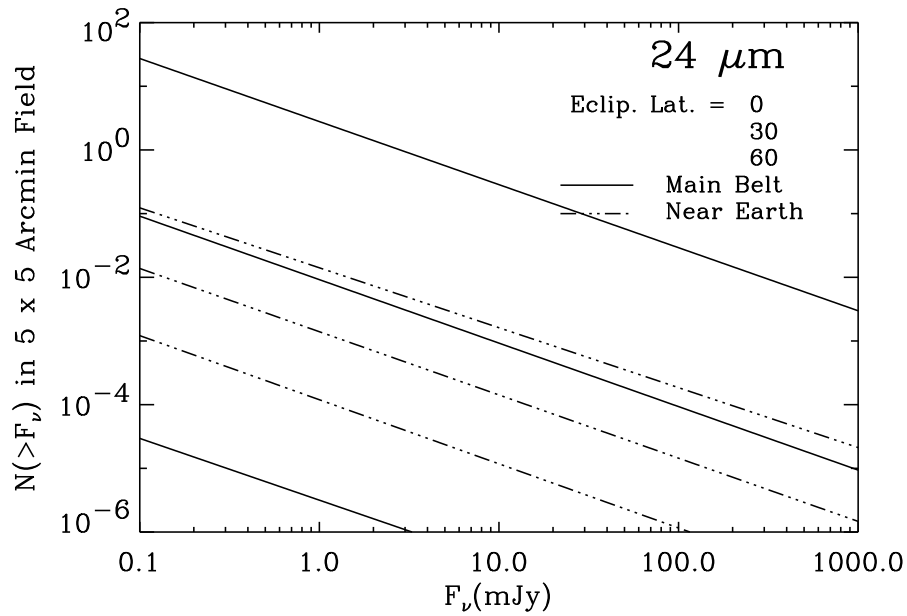


Fig. 1(f) - Same as Fig. 1(a) at 24  $\mu\text{m}$ .

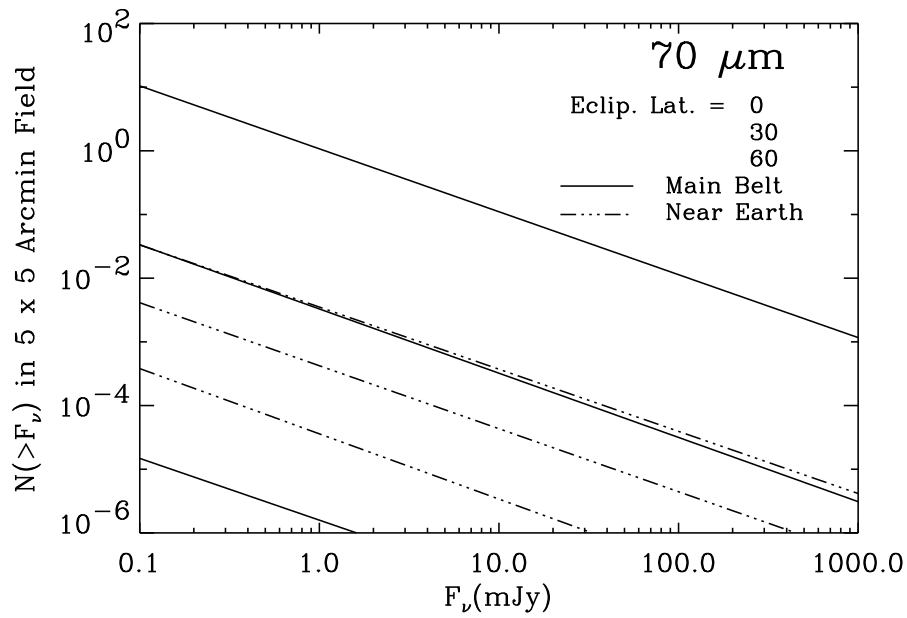


Fig. 1(g) - Same as Fig. 1(a) at 70  $\mu\text{m}$ .

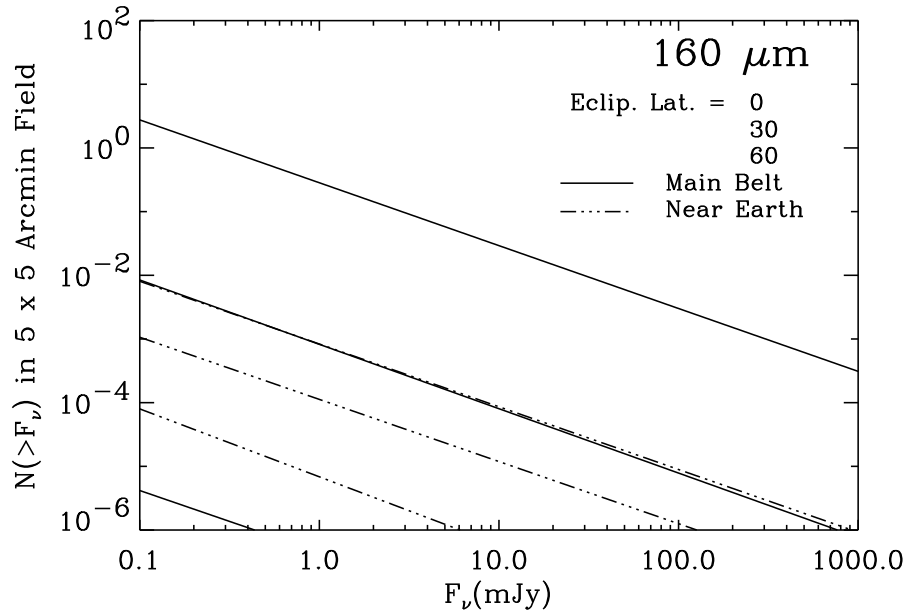


Fig. 1(h) - Same as Fig. 1(a) at 160  $\mu\text{m}$ .

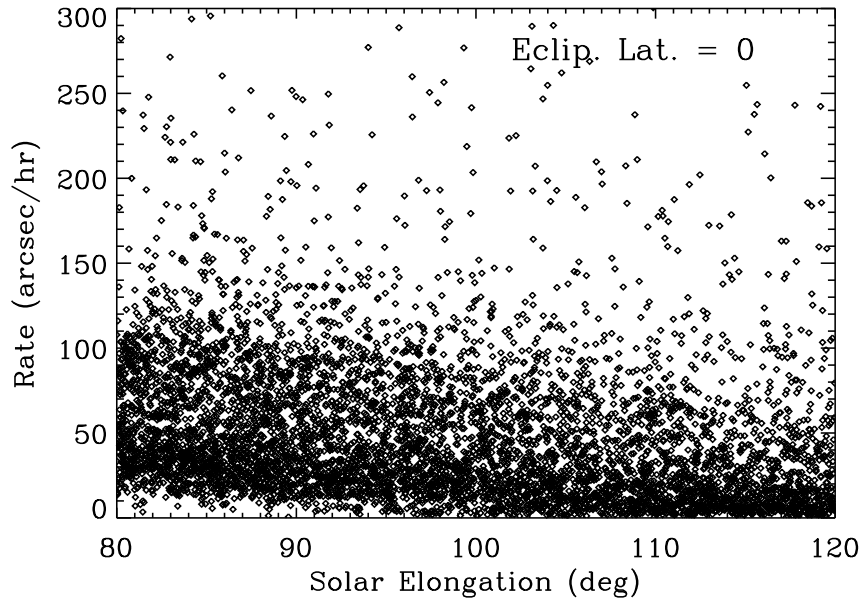


Fig. 2(a) - Simulation of the motions of near-earth asteroids in ecliptic coordinates as a function of solar elongation. Shown are 6390 objects with diameters greater than 60 m in a  $5^\circ$ -wide ecliptic latitude bin around  $0^\circ$ .

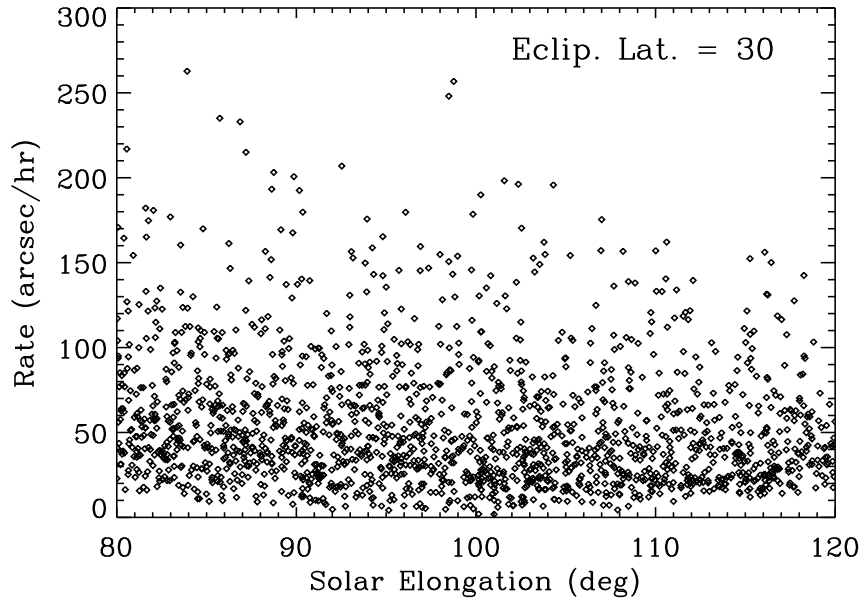


Fig. 2(b) - Same as Fig. 2(a) for 1745 objects in two  $2.5^\circ$ -wide ecliptic latitude bins around  $\pm 30^\circ$ .